

# Birth and metamorphoses of resonances in the driven van der Pol oscillator

Jan Kyzioł, Andrzej Okniński  
 Politechnika Świętokrzyska, Al. 1000-lecia PP 7,  
 25-314 Kielce, Poland

May 27, 2026

## Abstract

The dynamics of the driven van der Pol oscillator are investigated. We study birth and metamorphoses of 1 : 1 and 1 : 3 resonances within the formalism of differential properties of amplitude-frequency response implicit functions.

## 1 Introduction

We study the forced van der Pol equation in nondimensional form

$$\frac{d^2 z}{d\tau^2} - \mu(1 - z^2) \frac{dz}{d\tau} + z = F \cos(\Omega\tau), \quad (1)$$

where  $\tau$  is a nondimensional time and  $\mu$  is a positive damping parameter.

Equation (1) was introduced by van der Pol to describe vacuum-tube oscillations [1] (see also [2] for the non-forced equation). Investigations of vacuum-tube oscillations led to the early discovery of deterministic chaos, noticed by van der Pol and van der Mark in an electrical circuit described by Eq. (1) [3]. Equation (1) was investigated further by Cartwright and Littlewood [4] to confirm the presence of chaotic dynamics.

The van der Pol oscillator displays several generic nonlinear phenomena; see for global bifurcation phenomena Refs. [5–10].

The first application of the van der Pol oscillators outside electrical engineering, carried out by van der Pol and van der Mark, was to describe the heartbeat [11, 12]. Then, the van der Pol equation has been used to model self-sustained oscillations in physics, mechanics, engineering, and biology.

In this paper, we study birth and metamorphoses of 1 : 1 and 1 : 3 resonances in the framework of the differential properties of amplitude-frequency response implicit functions [14, 15], continuing our previous work on van der Pol-Duffing equation [16, 17].

## 2 Nonlinear resonances via KBM method

We apply the Krylov-Bogoliubov-Mitropolsky (KBM) perturbation approach [13] to Eq. (1). We assume a resonance in form

$$z_\alpha(\tau) = A \cos(\alpha\Omega\tau + \varphi) + \varepsilon z_1(A, \varphi, \tau) + \dots, \quad (2)$$

where the amplitude  $A$  and frequency  $\Omega$  fulfil the amplitude-frequency response equation

$$\mathcal{F}_\alpha(A, \Omega, \mu, F) = 0. \quad (3)$$

In what follows we consider  $\alpha = 1$  and  $\alpha = \frac{1}{3}$  for 1 : 1 and 1 : 3 resonances, respectively. In the case of primary resonance, we have

$$\mathcal{F}_{1:1}(A, \Omega, \mu, F) = A^2 \left( \mu^2 \Omega^2 \left(1 - \frac{1}{4}A^2\right)^2 + \left(1 + \frac{3}{4}\lambda A^2 - \Omega^2\right)^2 \right) - F^2, \quad (4)$$

while for the 1 : 3 resonance we get

$$\begin{aligned} \mathcal{F}_{1:3}(A, \Omega, \mu, F) = & \Omega^4 \mu^4 \left( A^2 - 4 + \frac{2F^2}{(\Omega^2 - 1)^2} \right)^2 + \Omega^2 \mu^2 \left( \frac{4}{3}\Omega^2 - 12 \right)^2 \\ & - \frac{\Omega^4 A^2 F^2 \mu^4}{(\Omega^2 - 1)^2} \quad (\Omega \neq 1). \end{aligned} \quad (5)$$

## 3 Singular and critical points of the amplitude profiles

Singular points of an implicit function  $L(A, \Omega, \underline{c}) = 0$ , where  $\underline{c} = c_1, c_2, \dots$  are parameters, are solutions of equations

$$L(A, \Omega, \underline{c}) = 0, \quad (6a)$$

$$\frac{\partial L(A, \Omega, \underline{c})}{\partial \Omega} = 0, \quad (6b)$$

$$\frac{\partial L(A, \Omega, \underline{c})}{\partial A} = 0. \quad (6c)$$

Solutions of Eqs. (6), if exist, are of form  $A = A_*$ ,  $\Omega = \Omega_*$ ,  $\underline{c} = \underline{c}_*$ .

It follows from Eqs. (6b) and (6c), that in the neighborhood of a singular point  $(A_*, \Omega_*)$  of the function  $L(A, \Omega, \underline{c}_*) = 0$ , neither of the functions  $\Omega = f(A)$  nor  $A = g(\Omega)$  is single-valued.

Moreover, equations (6a) and (6b) are conditions for extremas of the function  $A = g(\Omega)$ , while equations (6a), (6c) are conditions for vertical tangencies of the function  $A = g(\Omega)$  or extremas of the function  $\Omega = f(A)$ .

### 3.1 The case of resonance 1 : 1

To compute singular points of the amplitude-frequency implicit function for the 1 : 1 resonance, we substitute in (6)  $L(A, \Omega, \underline{c}) = \mathcal{F}_{1:1}(A, \Omega, \mu, F)$ .

Solutions of Eqs. (7)

$$\mathcal{F}_{1:1}(A, \Omega, \mu, F) = 0 \quad (7a)$$

$$\frac{\partial \mathcal{F}_{1:1}(A, \Omega, \mu, F)}{\partial A} = 0 \quad (7b)$$

$$\frac{\partial \mathcal{F}_{1:1}(A, \Omega, \mu, F)}{\partial A} = 0 \quad (7c)$$

read

$$A = 2, \Omega = 1, F = 0, \quad (\mu \neq 0) \quad (8)$$

and

$$\left. \begin{aligned} 5\mu^2 A^6 - 44\mu^2 A^4 + (-192 + 112\mu^2) A^2 + 256 - 64\mu^2 &= 0 \\ 8\Omega^2 + 16\mu^2 - 8\mu^2 A^2 + \mu^2 A^4 - 32 &= 0 \\ (\mu^4 - 5\mu^2) A^4 + (-120 + 38\mu^2 - 8\mu^4) A^2 - 104\mu^2 + 160 + 16\mu &= 5^3 F^2 \end{aligned} \right\} (9)$$

Solution (8) corresponds to an isolated point, while solution (9) represents self-intersections.

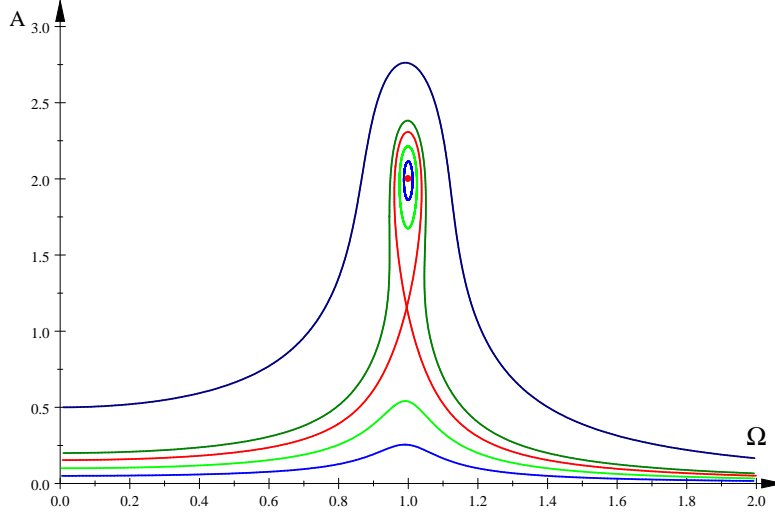


Figure 1: Amplitude-frequency response functions  $\mathcal{F}_{1:1}(A, \Omega, \mu, F) = 0$ .  $\mu = 0.2$ ;  $F = 0.05, 0.10, 0.153618, 0.20, 0.50$  (LightBlue, LightGreen, LightRed, Green, Blue). LightRed dot marks an isolated point.

Moreover, solutions of Eqs. (10) for vertical tangencies

$$\mathcal{F}_{1:1}(A, \Omega, \mu, F) = 0 \quad (10a)$$

$$\frac{\partial \mathcal{F}_{1:1}(A, \Omega, \mu, F)}{\partial A} = 0 \quad (10b)$$

are

$$\left. \begin{aligned} &2\mu^4 A^{12} + (-3F^2\mu^4 - 16\mu^4) A^{10} + (28F^2\mu^4 + 32\mu^4) A^8 \\ &+ (-80F^2\mu^4 + 32F^2\mu^2) A^6 + (64F^2\mu^4 - 128F^2\mu^2) A^4 + 128F^4 = 0 \\ &2A^6\mu^2 - (3F^2\mu^2 + 8\mu^2) A^4 + 16\mu^2 F^2 A^2 - 16F^2\mu^2 + 32F^2 = 16F^2\Omega^2 \end{aligned} \right\} \quad (11)$$

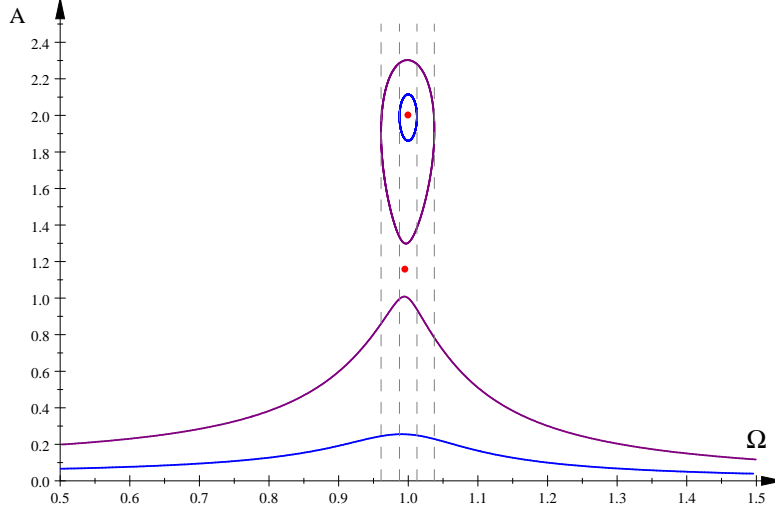


Figure 2: Amplitude-frequency response functions  $\mathcal{F}_{1:1}(A, \Omega, \mu, F) = 0$ .  $\mu = 0.2$ ;  $F = 0.05, 0.15$  (LightBlue, Purple). LightRed dots mark singular points. Dashed lines show vertical tangencies.

### 3.2 The case of resonance 1 : 3

Since the implicit function  $\mathcal{F}_{1:3}(A, \Omega, \mu, F) = 0$  depends on  $A^2$ ,  $\Omega^2$ ,  $\mu^2$ , and  $F^2$  only we write Eq. (5) in a simpler form

$$L_{1:3}(Y, X, m, f) = X^2 m^2 \left( Y - 4 + \frac{2f}{(X-1)^2} \right)^2 + X m \left( \frac{4}{3} X - 12 \right)^2 - \frac{X^2 Y f m^2}{(X-1)^2}, \quad (12)$$

where  $Y = A^2$ ,  $X = \Omega^2$ ,  $m = \mu^2$ ,  $f = F^2$ , and  $L_{1:3}(A^2, \Omega^2, \mu^2, F^2) = \mathcal{F}_{1:3}(A, \Omega, \mu, F)$ .

Singular points of the implicit function  $L_{1:3}(Y, X, m, f) = 0$  are solutions of the following equations

$$L_{1:3}(Y, X, m, f) = 0, \quad (13a)$$

$$\frac{\partial L_{1:3}(Y, X, m, f)}{\partial X} = 0, \quad (13b)$$

$$\frac{\partial L_{1:3}(Y, X, m, f)}{\partial Y} = 0. \quad (13c)$$

We note here that there are two kinds of singular points in these systems: isolated points and self-intersections. The isolated points are signatures of the birth of a new branch of solution, while self-intersections correspond to rupture of existing branches.

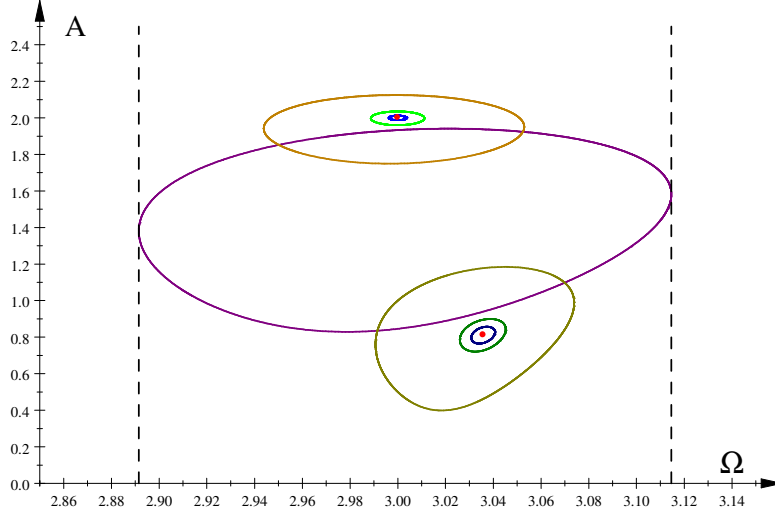


Figure 3: Amplitude-frequency response functions  $L_{1:3}(Y, X, m, f) = 0$ .  $\mu = 0.2$ ;  $F = 0.2, 0.6, 3, 8.7, 12, 12.25, 12.26$  (LightBlue, LightGreen, Sienna, Purple, Brown, Green, Blue). LightRed dots mark isolated points. Dashed lines show vertical tangencies.

Moreover, vertical tangencies are computed from

$$L_{1:3}(Y, X, m, f) = 0, \quad (14a)$$

$$\frac{\partial L_{1:3}(Y, X, m, f)}{\partial Y} = 0. \quad (14b)$$

Vertical tangencies show the range of a resonance, while self-intersections correspond to rupture of existing branches.

We solve Eqs. (13) to get the following singular solutions

$$X = 9, Y = 4, f = 0, \quad (m \text{ arbitrary}) \quad (15a)$$

which is an isolated point, and another solution

$$\begin{cases} Y = \frac{-5X^3 + 73X^2 + 12mX^2 - 243X - 81}{3mX^2}, \\ f = 4 \frac{-4354X^3 + 11732X^2 + 17010X + 3969 + 315X^4 + 108X^4m - 360X^3m - 324mX^2}{315mX^2}, \\ 175X^5 + (-216m - 3535)X^4 + (720m + 22498)X^3 \\ + (648m - 40194)X^2 - 31185X - 5103 = 0, \end{cases} \quad (15b)$$

with arbitrary  $m$ .

Condition that discriminant of equation for  $X$  in (15b) vanishes yields  $m = -28$ ,  $m = 0$ , and

$$\begin{aligned} 24564384m^4 + 1317273111m^3 + 104720016996m^2 \\ -1475275114404m - 178499175680 = 0. \end{aligned} \quad (16)$$

A positive solution of Eq. (16) is  $m_{cr} = 12.009279$ . Accordingly, equation for  $X$  in Eq. (15b) has one positive root for  $m < m_{cr}$ , corresponding to an isolated point, and three positive roots for  $m > m_{cr}$ , corresponding to two isolated points and one self-intersection.

To compute vertical tangencies, we solve equations (14) obtaining

$$Y = \frac{8X^2 - 16X - 3f + 8}{2(1-X)^2}, \quad (17a)$$

$$\begin{aligned} 64X^6 - 1408X^5 + 10176X^4 + (-27904 - 144mf)X^3 \\ + (35776 + 288mf)X^2 + (63mf^2 - 21888 - 144mf)X + 5184 = 0. \end{aligned} \quad (17b)$$

In the case when two vertical tangencies overlap, we have a singular point – an isolated point. This happens when Eq. (17b) has a double root, i.e. when a discriminant,  $D(m, f)$ , of Eq. (17b) vanishes. Computing the discriminant, we get

$$D = \left( \begin{array}{l} 987614208m^4f^4 - 4514807808f^3m^4 + 5159780352f^2m^4 \\ + 27205113600m^3f^4 - 30059237376m^3f^3 - 1056502185984f^2m^3 \\ + 761014517760fm^3 - 472696875f^5m^2 + 96981192000m^2f^4 \\ - 3830568505344m^2f^3 - 11576272748544m^2f^2 - 60542932746240fm^2 \\ - 22265110462464m^2 - 55535398912f^3m - 11861638512640mf^2 \\ + 263571835034096mf + 2216615441596416m + 377132488327168f \\ - 55169095435288576 \end{array} \right) \quad (18)$$

The plot of  $D(m, f) = 0$  is shown in Fig. 4. Figure 4 shows values of parameters  $f, m$  for which the function  $L(Y, X, m, f) = 0$  has singular (isolated) points (red and blue curves). Values of  $f$  and  $m$  that lead to physical values for  $X$  and  $Y$  are on the red interval.

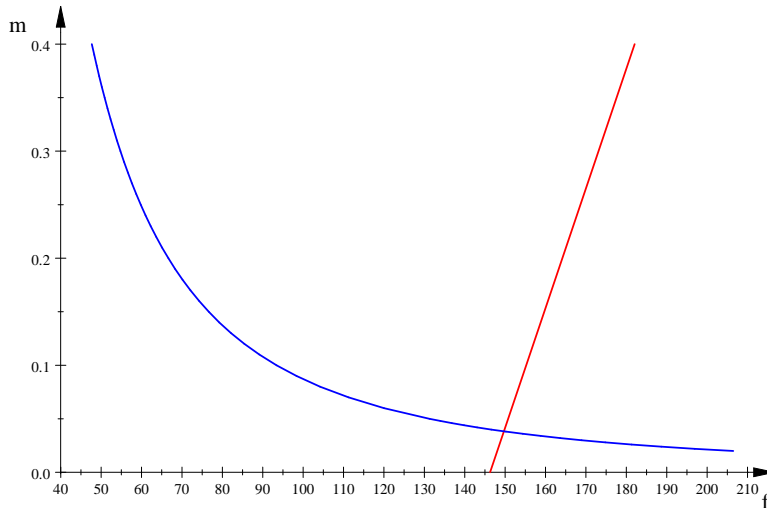


Figure 4: Manifold of singular (isolated) points. Physical points lie on the LightRed interval. .

## 4 Computational results

In this Section, we numerically solve Eq. (1) and compare the results with analytical predictions.

### 4.1 The case of resonance 1 : 1

The solution (8) of Eqs. (7) describes a well-known limit cycle of the unforced van der Pol equation [10]. This solution is a good approximation to the limit cycle for small  $\mu$ , while for large values of  $\mu$  a good approximation can be found in [18, 19].

It follows from Figs. 1 and 2 that for  $F < 0.153618$  the amplitude-frequency response function for the 1 : 1 resonance consists of two disjoint pieces, where, as we were able to determine, only the upper part is stable.

We have solved Eqs. (10) for vertical tangencies setting  $\mu = 0.2$  and  $F = 0.05$ , and  $F = 0.15$ . We have obtained  $\Omega_1 = 0.987395$ ,  $A_1 = 1.991838$  and  $\Omega_2 = 1.012447$ ,  $A_2 = 1.992244$  for  $F = 0.05$  and  $\Omega_1 = 0.960887$ ,  $A_1 = 1.905297$  and  $\Omega_2 = 1.037503$ ,  $A_2 = 1.921864$  for  $F = 0.15$ .

In Fig. 2, the computed vertical tangencies are shown. The corresponding upper parts of the amplitude profiles are in the intervals  $(\Omega_1, \Omega_2)$ .

We have solved Eq. (1) numerically for  $\mu = 0.2$  and  $F = 0.05$ , and  $F = 0.15$ ; see Fig. 5 for the corresponding bifurcation diagrams. We have determined that for  $F = 0.05$ , the 1 : 1 resonance exists in the interval  $\Omega \in (0.9848, 1.0104)$ ,

while for  $F = 0.15$  the primary resonance is in the interval  $\Omega \in (0.9589, 1.0355)$ . We notice a good agreement between numerical and analytical results.

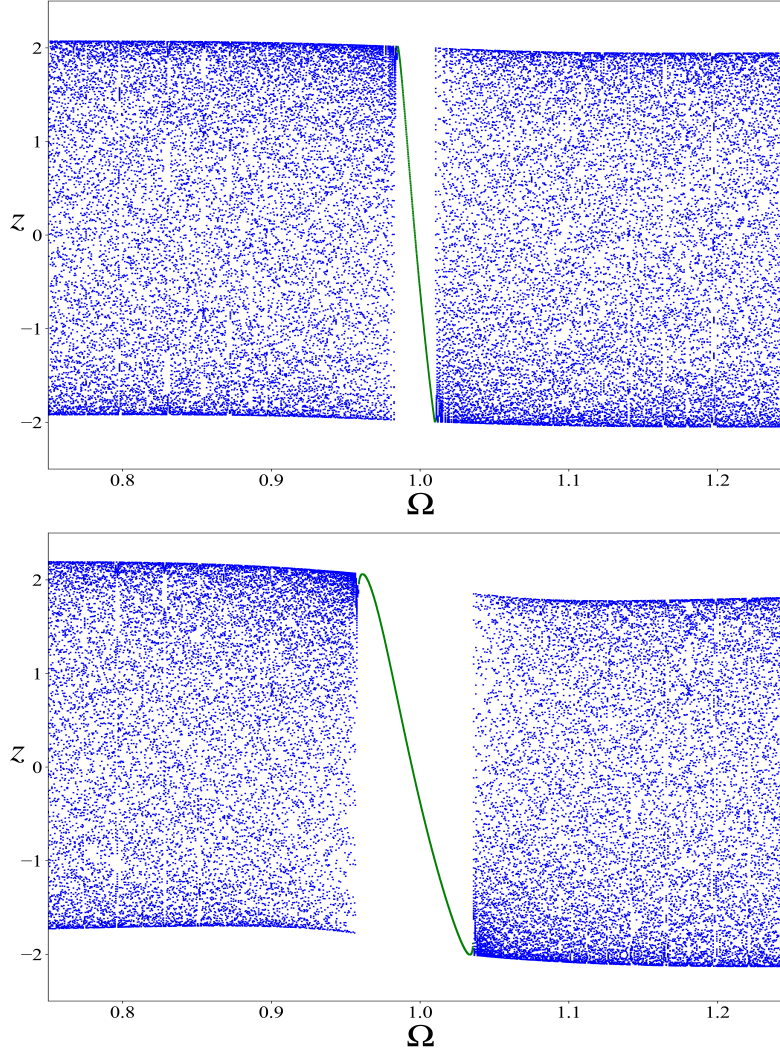


Figure 5: The birth and growth of 1 : 1 resonance (Green) – numerical solutions of Eq. (1).  $\mu = 0.2$ ;  $F = 0.05$  (top),  $0.15$  (bottom). Chaotic dynamics is Blue.

## 4.2 The case of resonance 1 : 3

We have solved Eqs. (13) choosing  $m = 0.04$  ( $\mu = 0.2$ ) obtaining two singular solutions  $X = \Omega^2 = 9$ ,  $Y = A^2 = 4$ , and  $f = F^2 = 0$ , and  $X = 9.216088$ ,

$Y = 0.658061$ , and  $f = 150.396416$ . Both solutions correspond to isolated points.

The first isolated point corresponds to the birth of 1 : 3 resonance; see Figs. 6, while the second isolated point corresponds to its decay; see Figs. 8 and 9.

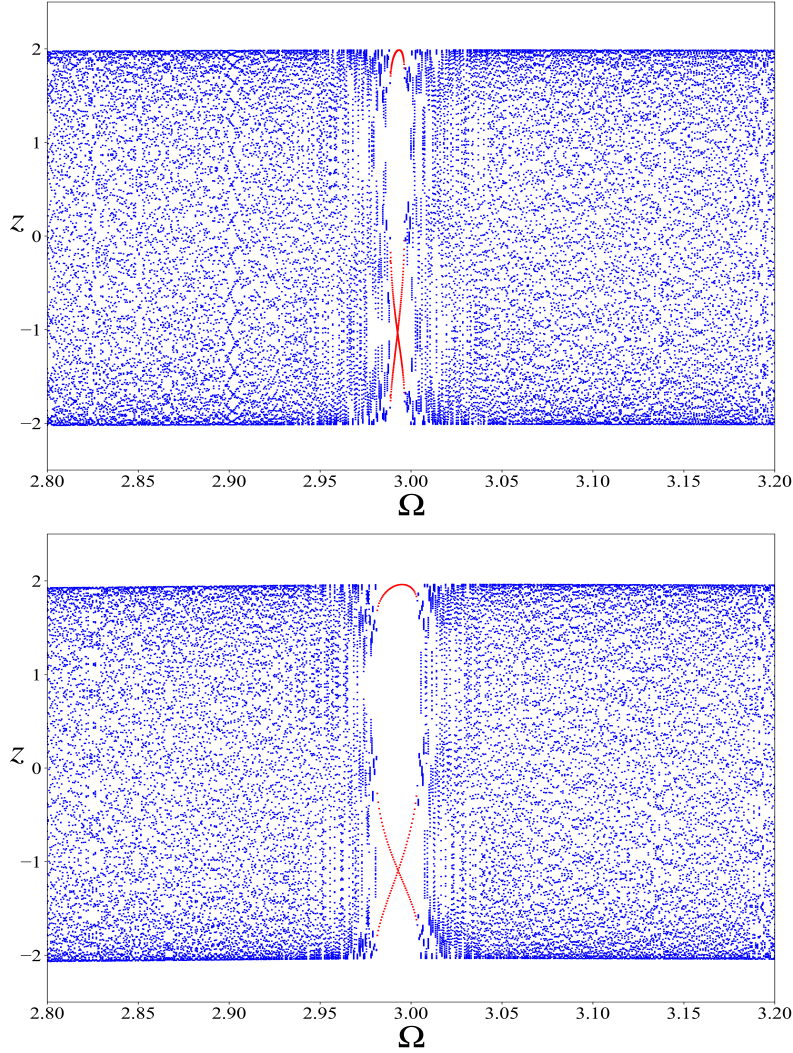


Figure 6: The birth and growth of 1 : 3 resonance (Red) – numerical solutions of Eq. (1).  $\mu = 0.2$ ;  $F = 0.2$  (top), and  $F = 0.6$  (bottom). Chaotic dynamics is Blue.

We have also solved Eqs. (14) choosing  $m = 0.04$  and  $f = 75.69$  ( $F = 8.7$ ) obtaining two vertical tangencies,  $X_1 = 8.360693$ ,  $Y_1 = 1.904477$  and  $X_2 = 9.700773$ ,  $Y_2 = 2.500266$ ;  $\Omega_1 = \sqrt{X_1} = 2.891486$ ,  $\Omega_2 = \sqrt{X_2} = 3.114606$ .

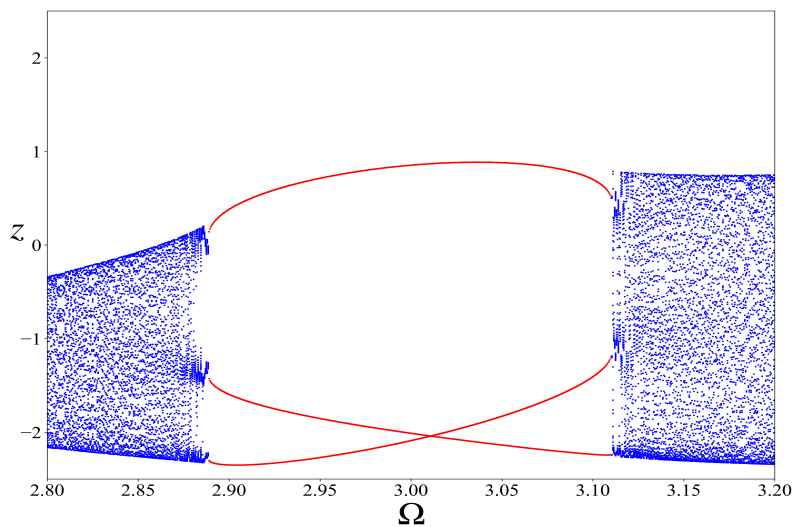


Figure 7: The fully developed 1 : 3 resonance (Red) – numerical solution of Eq. (1).  $\mu = 0.2$ ;  $F = 8.7$ . Chaotic dynamics is Blue.

Figure 7 shows a fully developed 1 : 3 resonance. Positions of the computed vertical tangencies, determining the beginning and the end of the resonance, agree well with Fig. 7 – the resonance is in the interval  $\Omega \in (2.8890, 3.1100)$ .

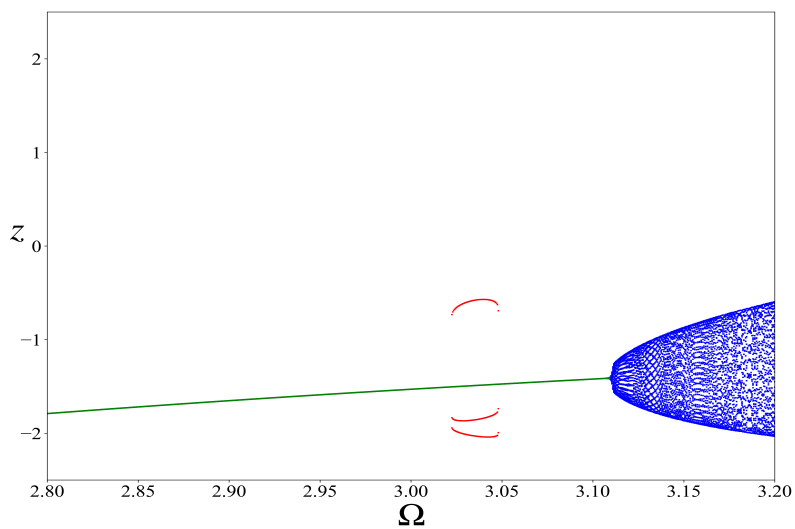


Figure 8: The decay of 1 : 3 resonance (Red) – numerical solution of Eq. (1).  $\mu = 0.2$ ;  $F = 12.25$ . 1 : 1 resonance is Green, chaotic dynamics is Blue.

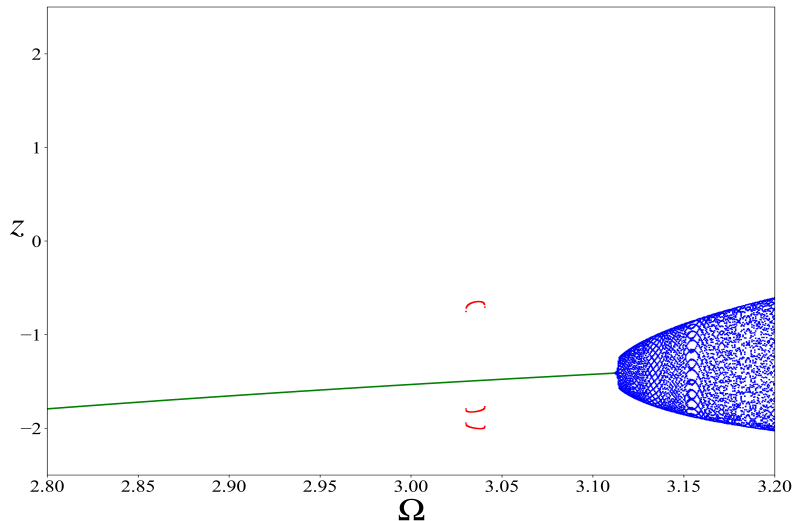


Figure 9: The decay of 1 : 3 resonance (Red) – numerical solution of Eq. (1).  $\mu = 0.2$ ;  $F = 12.27$ . 1 : 1 resonance is Green, chaotic dynamics is Blue.

Figures 8 and 9 show decay of the 1 : 3 resonance. The resonance disappears completely for  $F = 12.28$ , which agrees well with the computed value of  $F$  for the second singular point,  $F = \sqrt{150.396416} = 12.263622$ .

## 5 Summary

In this work, we have studied the formation and growth of 1 : 1 and 1 : 3 resonances in the forced van der Pol oscillator, Eq. (1). Our approach consists of applying the geometry of algebraic curves to investigate differential properties of amplitude-frequency (implicit) response functions [14,15]. More precisely, we have studied response functions for the 1 : 1 and 1 : 3 resonances; see Eqs. (4) and (5), respectively, computed singular points and vertical tangencies of these functions, using Eqs. (6) (i.e., Eqs. (7) or (13)) as well as Eqs. (6a) and (6c) (i.e., Eqs. (10) or (14)).

Isolated singular points correspond to the birth of a new branch of solution, while vertical tangencies let us estimate the width of a resonance.

We have obtained the following results.

1. In the case of the response function for the 1 : 1 resonance, the computed isolated point signals formation of the resonance, recovering a well-known result, reasonably exact for small value of  $\mu$  [10]. Moreover, the computed vertical tangencies permit the prediction of the width of the growing resonance with good precision.

2. In the case of the response function for the 1 : 3 resonance, the computed isolated points show the birth as well as decay of the resonance with good precision. Moreover, the computed vertical tangencies provide a good estimate of the width of the resonance.

## 6 Computational details

Nonlinear polynomial equations were solved numerically using the computational engine Maple from Scientific WorkPlace 5.5. Figures 1, 2, 3, and 4 were plotted with the computational engine MuPAD from Scientific WorkPlace 5.5. Curves shown in bifurcation diagrams in Figs. 5, 6, 7, 8, and 9 were computed and plotted running DYNAMICS, a program written by Helena E. Nusse and James A. Yorke [20], as well as our own programs, written in Pascal and Python [21].

## References

- [1] B. van der Pol, Forced Oscillations in a Circuit with Nonlinear Resistance, *The London, Edinburgh, and Dublin Philosophical Magazine and Journal of Science Ser. 7*, **3**(13) (1927) 65-80.
- [2] B. van der Pol, On Relaxation-Oscillations, *The London, Edinburgh, and Dublin Philosophical Magazine and Journal of Science Ser. 7*, **2**(11) (1926) 978-992.
- [3] B. van der Pol and J. van der Mark, Frequency Demultiplication, *Nature* **120** (1927) 363-364.
- [4] M.L. Cartwright and J.E. Littlewood, On non-linear differential equations of the second order. I. The equation  $\ddot{y} - k(1 - y^2)\dot{y} + y = b\lambda k \cos(\lambda t + a)$ ,  $k$  - large, *J. London Math. Soc.* **20** (1945) 180-189.
- [5] P.J. Holmes and D.A. Rand, Bifurcations of the forced van der Pol oscillator, *Quart. Appl. Math.* **35** (1978) 495-509.
- [6] U. Parlitz and W. Lauterborn, Period-doubling cascades and devil's staircases of the driven van der Pol oscillator, *Phys. Rev. A* **36**(3) (1987) 1428-1434.
- [7] R. Mettin, U. Parlitz, and W. Lauterborn, Bifurcation structure of the driven van der Pol oscillator, *Int. J. Bifur. Chaos* **3**(6) (1993) 1529-1555.
- [8] J. Guckenheimer, K. Hoffman, and W. Weckesser, The Forced van der Pol Equation I: The Slow Flow and Its Bifurcations, *SIAM J. Appl. Dyn. Systems* **2**(1) (2003) 1-35.
- [9] K. Bold et al., The Forced van der Pol Equation II: Canards in the Reduced System, *SIAM J. Appl. Dyn. Systems* **2**(4) (2003) 570-608.

- [10] D.W. Jordan and P. Smith, *Nonlinear Ordinary Differential Equations*, 4th Edition, Oxford University Press, Oxford, New York 2007.
- [11] B. van der Pol and J. van der Mark, The heartbeat considered as a relaxation oscillation, and an electrical model of the heart, *The London, Edinburgh, and Dublin Philosophical Magazine and Journal of Science Ser. 7*, **6**(38) (1928) 763-785.
- [12] A. Pikovsky, M. Rosenblum, J. Kurths, *Synchronization: A Universal Concept in Nonlinear Sciences*, Cambridge University Press, Cambridge, New York, Melbourne, Madrid, Cape Town, Singapore, São Paulo 2001.
- [13] A.H. Nayfeh, *Introduction to Perturbation Techniques*, John Wiley & Sons, 2011.
- [14] C.G. Gibson, *Elementary Geometry of Algebraic Curves: An Undergraduate Introduction*, Cambridge University Press, Cambridge 1998.
- [15] J. Kyzioł and A. Okniński, Localizing Bifurcations in Non-Linear Dynamical Systems via Analytical and Numerical Methods, *Processes* **10**(1) (2022) 127 (17 pages).
- [16] J. Kyzioł and A. Okniński, The Duffing–Van der Pol Equation: Metamorphoses of Resonance Curves, *Nonlinear Dynamics and Systems Theory* **15**(1) (2015) 25–31.
- [17] J. Kyzioł and A. Okniński, Van der Pol-Duffing oscillator: Global view of metamorphoses of the amplitude profiles, *International Journal of Non-Linear Mechanics* **116** (2019) 102–106.
- [18] A.A. Dorodnicyn, Asymptotic solution of van der Pol’s equation, *Prikl. Math. I. Meh.* **11** (1947) 313-328; *Am. Math. Soc. Translation number 88* (1953).
- [19] J. A. Zonneveld, Periodic solutions of the Van der Pol equation, *Nederl. Akad. Wetensch. Proc. Ser. A 69=Indag. Math.*, **28** (1966), 620–622
- [20] H.E. Nusse and J.A. Yorke, *Dynamics: Numerical Explorations: Accompanying Computer Program Dynamics*, Vol. 101, Springer, New York.
- [21] F. Pérez, and B.E. Granger, 2007, Ipython: A System for Interactive Scientific Computing, *Comput. Sci. Eng.*, **9**(3), pp. 21–29.